 doi:10.20944/preprints202105.0421.v1

Unveiling the Different Reactivity of Bent and Linear Three-Atom-Components Participating in [3+2] Cycloaddition Reactions

Mar Ríos-Gutiérrez,*[a] Luis R. Domingo,[a] Fatemeh Ghodsi[b]

[a] Department of Organic Chemistry, University of Valencia, Dr Moliner 50, 46100 Burjassot, Valencia, Spain
[b] Department of Chemistry, University of Sistan and Baluchestan, Zahedan, Iran

email: rios@utopia.uv.es

Abstract

The 32CA reactions of a series of pairs of bent three-atom-component (B-TACs) and linear TACs (L-TACs) towards electrophilic dicyanoethylene (DCE) have been studied within the Molecular Electron Density Theory in order to understand their different reactivity. ELF analysis indicates that while *pseudodiradical* B-TACs change their electronic structure to *pseudoradical* or carbenoid L-TACs upon dehydrogenation, zwitterionic B-TACs experience no remarkable change. Analysis of the CDFT indices indicates that five of the nine studied TACs have a strong nucleophilic character, thus participating in polar reactions towards electrophilic ethylenes. The activation energies of the 32CA reactions of the nine TACs towards electrophilic DCE range from 0.5 to 22.0 kcal·mol^{-1}, which are by between 4.3 and 9.1 kcal·mol^{-1} lower than those involved in the non-polar 32CA reactions with ethylene. In general, B-TACs are more reactive than their L-TAC counterparts. A change of the regioselectivity is found in these polar 32CA reactions; in general, while B-TACs are *meta* regioselective, L-TACs are *ortho* regioselective. Analysis of the geometrical parameters indicates that at all TSs, the formation of the single bond involving the most electrophilic C4 carbon of DCE is more advanced than that involving the C5 one. A change of the asynchronicity in the reactions involving B-TACs and L-TACs is also found.

Keywords: [3+2] cycloaddition reactions, bent and linear three-atom-components, reactivity, regioselectivity, molecular electron density theory.

Preprints (www.preprints.org) | NOT PEER-REVIEWED | Posted: 18 May 2021 doi:10.20944/preprints202105.0421.v1

1. Introduction

Cycloaddition reactions are one of the most useful tools in organic synthesis as they permit to obtain cyclic compounds with a regio- and/or stereoselective fashion [1,2]. [3+2] cycloaddition (32CA) reactions are an important type of cycloadditions allowing the formation of five-membered heterocycles of great pharmaceutical and industrial interest [2,3]. This kind of cycloaddition implicates the 1,3-addition of an ethylene derivative to a three-atom-component (TAC) (see Scheme 1).

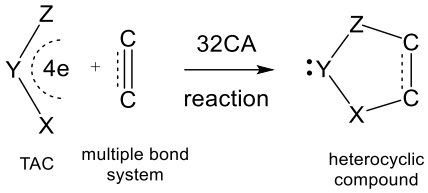

Scheme 1. 32CA reaction between a TAC and an ethylene derivative.

Recent advances made in the theoretical understanding of 32CA reactions based on Molecular Electron Density Theory [4] (MEDT) have allowed establishing a very good correlation between the electronic structure of TACs and their reactivity [5]. Thus, depending on the electronic structure of TACs, *pseudodiradical*, *pseudo(mono)radical*, carbenoid and zwitterionic, 32CA reactions have been classified into *pseudodiradical*-type *(pdr-type)*, *pseudomonoradical*-type *(pmr-type)*, carbenoid-type (*cb-type)* and zwitterionic-type *(zw-type)* reactions [5], in such a manner that while *pdr-type* 32CA reactions can be carried out very easily, *zw-type* 32CA reactions demand adequate nucleophilic/electrophilic activations to take place (see Scheme 2).

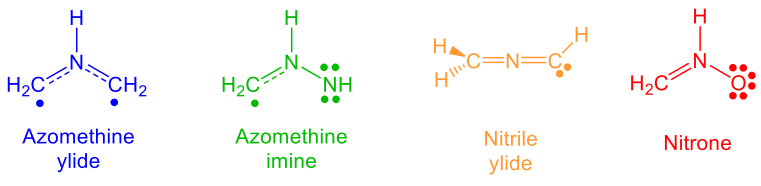

Structure			
pseudodiradical	*pseudoradical*	carbenoid	zwitterionic
Reactivity			
pdr-type	*pmr-type*	*cb-type*	*zw-type*

Scheme 2. The four representative reactivity models in 32CA reactions

Preprints (www.preprints.org) | NOT PEER-REVIEWED | Posted: 18 May 2021 doi:10.20944/preprints202105.0421.v1

Organic reactions can also be classified as non-polar and polar reactions, in such a way that organic reactions are favoured with the increase of the polar character of the reaction [6]. In 2014, Domingo proposed the analysis of the global electron density transfer (GEDT) [7,8] at the transition state structures (TSs) as a measure of the polar character of a reaction. Reactions with GEDT values below 0.05 e correspond to non-polar processes, while values above 0.20 e correspond to polar processes. Very recently, organic reactions have been classified as forward electron density flux (FEDF) and reverse electron density flux (REDF) reactions, depending on the direction of the flux of the electron density at the TS [9]. Non-polar reactions are classified as null electron density flux (NEDF) reactions [10]. This classification is unequivocal, as the GEDT is a measure of the actual electron density transfer at the TSs. Thus, while the DA reaction between butadiene and ethylene was classified as "normal electron demand" [11] within Sustmann's classification [12], it is classified as an NEDF reaction because of its non-polar character; note that the GEDT at this DA reaction is negligible, 0.0 e [13].

TACs can also be classified as bent TACs (B-TACs), such as azomethine ylide, and linear TACs (L-TACs), such nitrile ylide (see Scheme 2), depending on their geometrical structure. In many cases, a close relation between B-TACs and L-TACs can be established, as L-TACs can be considered resulting from the dehydrogenation of B-TACs (see Scheme 3). As the dehydrogenation of B-TACs involves the loss of the hydrogen of the central Y atom of the TAC, this atom changes the trigonal arrangement at the B-TAC to a linear one at the L-TAC, thus justifying the change of the geometry of the TACs.

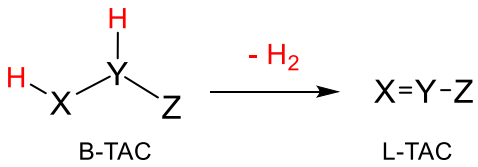

Scheme 3. Chemical relationships between some B- and L-TACs.

In general, considering a B-TAC/L-TAC pair, B-TACs are more reactive and the 32CA reactions towards electrophilic ethylenes are more regioselective than those involving L-TACs. In order to establish some general correlations between the structure and reactivity of B- and L-TACs, a MEDT study of the 32CA reactions of five pairs of B-TACs **1**-**4** and L-TACs **5**-**8** (see Table 1) with ethylene **9** and the electrophilic dicyanoethylene (DCE) **10** is herein carried out.

Preprints (www.preprints.org) | NOT PEER-REVIEWED | Posted: 18 May 2021 doi:10.20944/preprints202105.0421.v1

Table 1. Atom composition and name of the pairs of B- and L-TACs herein studied.

B-TACs			L-TACs		
	X1–N2–Z3	Name		X1–N2–Z3	Name
1	$H_2C{-}NH{-}CH_2$	azomethine ylide	**5**	$H_2C{-}N{-}CH$	nitrile ylide
2	$H_2C{-}NH{-}NH$	azomethine imine	**61**	$H_2C{-}N{-}N$	diazomethane
			62	$HC{-}N{-}NH$	nitrile imine
3	$NH{-}NH{-}NH$	azimine	**7**	$NH{-}N{-}N$	azide
4	$H_2C{-}NH{-}O$	nitrone	**8**	$HC{-}N{-}O$	nitrile oxide

2. Computational Methods

All stationary points were optimised using the MPWB1K functional [14], together with the 6-311G(d,p) basis set [15]. The optimisations were carried out using the Berny analytical gradient optimisation method [16,17]. The stationary points were characterized by frequency computations in order to verify that TSs have one and only one imaginary frequency. The intrinsic reaction coordinate (IRC) paths [18] were traced in gas phase in order to check and obtain the energy profiles connecting each TS to the two associated minima of the proposed mechanism, i.e. reactants and products, using the second order González-Schlegel integration method [19,20].

The electronic structures of the reagents were characterized by the topological analysis of the electron localisation function [21] (ELF) and by a Natural Population Analysis (NPA) [22,23]. CDFT reactivity indices [24,25] were computed at the B3LYP/6-31G(d) level as original reactivity scales were established at that method, using the equations given in reference 25. The GEDT [7] was computed by the sum of the atomic charges (q) of the atoms belonging to each framework at the TSs; GEDT = Σq_f. All computations were carried out with the Gaussian 16 suite of programs [26]. ELF studies were performed with the TopMod program [27], using the corresponding MPWB1K /6-311G(d,p) monodeterminantal wavefunctions and considering the standard cubical grid of step size of 0.1 Bohr. The molecular geometries and ELF basin attractor positions were visualised using the GaussView program [28].

3. Results and discussion

The present work has been divided into three sections: i) first, the electronic structures of B-TACs and L-TACs based on the topological analysis of the ELF and the NPA are compared; ii) then, the CDFT indices of the B-TACs and L-TACs are analysed in order

Preprints (www.preprints.org) | NOT PEER-REVIEWED | Posted: 18 May 2021 doi:10.20944/preprints202105.0421.v1

to understand their participation in polar 32CA reactions; and finally, iii) the non-polar and polar 32CA reactions of the nine TACs **1**-**8** with ethylene **9** and DCE **10** are explored in order to compare the reactivity of B-TACs and L-TACs.

3.1. Comparison of the electronic structures of B-TACs and L-TACs

The electron density distribution of matter determines both its physical and chemical properties, i.e. reactivity [4]. An appealing procedure that provides a straightforward connection between the electron density distribution and the chemical structure is the quantum chemical topological analysis of the ELF [21]. Hence, a topological analysis of the ELF and a NPA [22,23] of the nine selected TACs was performed in order to characterize the structural changes between the B-TAC/L-TAC pairs. ELF basin attractor positions and populations of the valence basins are given in Figure 1.

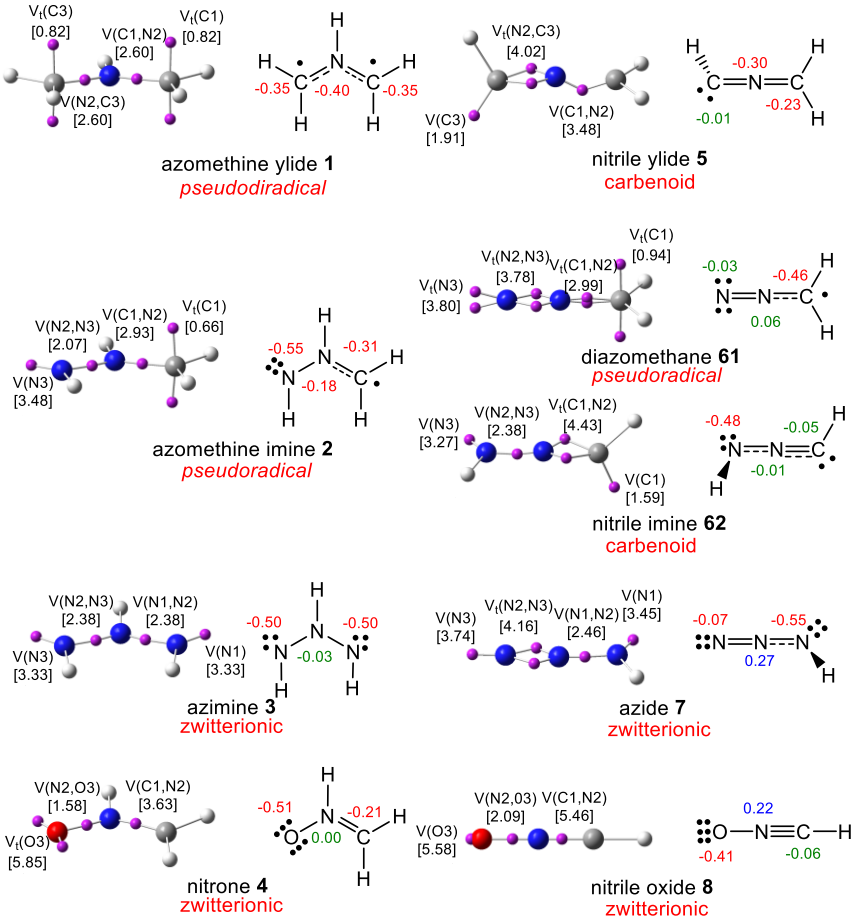

Figure 1. ELF basin attractor positions, ELF-based Lewis-like structures and TAC types, together with calculated natural atomic charges, in average number of electrons e, of TACs **1** - **8**. Negative charges are coloured in red, positive charges in blue, and negligible charges in green.

Preprints (www.preprints.org) | NOT PEER-REVIEWED | Posted: 18 May 2021 doi:10.20944/preprints202105.0421.v1

Azomethine ylide **1** is a *pseudodiradical* B-TAC characterized by the presence of two carbon *pseudoradical* centers (see the two V_t(C1[3]) monosynaptic basins integrating a total of 0.82 e each one in Figure 1), which are responsible for its high reactivity in *pdr-type* 32CA reactions even with low polar character, and two overpopulated C1[3]–N2 single bonds. After dehydrogenation of B-TAC **1**, the electron density at nitrile ylide **5** is redistributed into a carbenoid allenic linear structure characterized by the presence of a non-bonding electron density at the C3 carbon integrating 1.91 e (see the V(C3) monosynaptic basin in Figure 1) and two non-conjugated C1[3]–N2 double bonds. Thus, nitrile ylide **5** is characterised as a carbenoid L-TAC.

The ELF of B-TAC azomethine imine **2** shows a *pseudoradical* C1 carbon (see the two V(C1) monosynaptic basins integrating a total of 0.66 e in Figure 1) an C1–N2 overpopulated single bond and an N2–N3 single bond, thus indicating that **2** is a *pseudo(mono)radical* allylic B-TAC. Dehydrogenation of **2** can lead to two different L-TACs depending on which of the two C1–N2 or N2–N3 bonding regions is involved; dehydrogenation at the N2–N3 region gives rise to L-TAC diazomethane **61**, while dehydrogenation at the C1–N2 region yields L-TAC nitrile imine **62**. ELF shows that, upon dehydrogenation of the N2–N3 region, the freed electron density of diazomethane **61** has mainly been redistributed into the N2–N3 region, so that this L-TAC has a rather allenic, but still *pseudo(mono)radical*, structure (see the two V(C1) monosynaptic basins integrating a total of 0.94 e in Figure 1). On the other hand, at nitrile imine **62** the electron density freed upon dehydrogenation of the C1–N2 region is shared between that region and the C1 carbon. As a consequence, nitrile imine **62** presents the structure of a carbenoid L-TAC with a non-bonding electron density of 1.59 e at the carbenoid C1 carbon (see the V(C1) monosynaptic basin in Figure 1), and an N2–C3 double bond.

The electron density of B-TAC azimine **3** is distributed among two N1[3]–N2 single bonds integrating 2.38 e, and two terminal N1[3] nitrogen nuclei having a non-bonding electron density of 3.33 e each one. Given the absence of any *pseudo(mono)radical* or carbenoid center, azimine **3** should be characterized as a zwitterionic TAC. However, note that this TAC does not present any multiple bond. After dehydrogenation of **3**, the electron density of azide **7** is mainly redistributed into the N2–N3 bonding region, which becomes a double bond; therefore azide **7** keeps being characterized as a zwitterionic L-TAC.

Preprints (www.preprints.org) | NOT PEER-REVIEWED | Posted: 18 May 2021 doi:10.20944/preprints202105.0421.v1

Finally, nitrone **4** is a zwitterionic allylic B-TAC as it has no carbenoid or *pseudoradical* centers but an N2–C3 double bond. After dehydrogenation of **4**, the only noticeable structural change observed in nitrile oxide **8** is that the N2–C3 bonding region becomes a triple bond, so that L-TAC **8** keeps a zwitterionic structure. It can be inferred from this that the 2 e freed upon dehydrogenation of **4** have almost entirely been redistributed into the N2–C3 region.

The present topological analysis of the ELF at the ground state of the selected TACs shows that while some pairs of B-TACs and L-TACs keep the same structural type, such as zwitterionic **4**/**8** and **3**/**7**, and *pseudo(mono)radical* **2**/**61**, others change their structure, such as *pseudodiradical* **1** vs carbenoid **5**, and *pseudo(mono)radical* **2** vs carbenoid **62**.

On the other hand, NPA of the total formal charge at the X1–N2–Y3 core framework of the nine TACs shows that for the B-TACs it ranges from −1.10 e (**1**) to –0.72 e (**4**), while for the L-TACs it ranges from –0.55 e (**5**) to –0.36 e (**7**). These values clearly emphasize that the electronic structure of TACs cannot be considered the result of a set of resonance Lewis structures built from integer electron pairs [5], but the result of the distribution of the whole molecular electron density depending on the nature and relative positions of the different nuclei forming the TAC. Thus, as the nuclei are more electronegative that the hydrogen, the core frameworks of the nine TACs are negatively charged; the ones of B-TACs more than those of the dehydrogenated L-TACs as the former have more hydrogen atoms. Thus, while azomethine ylide **1** is the TAC with the most negatively charged core framework, –1.10e, as it has 5 hydrogens, nitrile oxide **8** is the TAC with the least negatively charged core structure, –0.25 e, as it has only one hydrogen. Consequently, the traditional definition of TACs as 1,3-dipoles mainly described by 1,2-zwitterionic Lewis structures [28] should be completely avoided [5].

3.2. Analysis of CDFT reactivity indices at the reagents

Numerous studies devoted to cycloaddition reactions have shown that the reactivity indices defined within CDFT [24,25] are a powerful tool to predict and understand organic chemical reactivity. Thus, in order to obtain some insight about the reactivity differences between B-TACs and L-TACs in 32CA reactions, the global CDFT indices, namely, the electronic chemical potential μ, the chemical hardness, η, the electrophilicity, ω, and the nucleophilicity, *N*, at TACs **1**-**8**, ethylene **9** and DCE **10**, were computed and

Preprints (www.preprints.org) | NOT PEER-REVIEWED | Posted: 18 May 2021 doi:10.20944/preprints202105.0421.v1

analysed (see Table 2). The CDFT indices were calculated at the B3LYP/6-31G(d) computational level since it was used to define the original electrophilicity and nucleophilicity scales [25].

Table 2. B3LYP/6-31G(d) global electronic chemical potential, μ, chemical hardness, η, electrophilicity, ω, and nucleophilicity, *N*, in eV, of simplest TACs **1-8**, ethylene **9** and DCE **10**.

	μ	η	ω	*N*
TAC **1**	-1.81	4.47	0.37	5.07
TAC **2**	-2.70	5.02	0.72	3.92
TAC **3**	-3.70	5.62	1.22	2.61
TAC **4**	-3.43	5.54	1.06	2.92
TAC **5**	-2.90	5.45	0.77	3.50
TAC **61**	-3.64	4.73	1.40	3.11
TAC **62**	-3.54	5.87	1.07	2.64
TAC **7**	-4.24	6.54	1.37	1.62
TAC **8**	-3.40	7.94	0.73	1.75
Ethylene **9**	-3.37	7.77	0.73	1.87
DCE **10**	-5.64	5.65	2.82	0.65

The electronic chemical potentials [24] μ of TACs range from −1.81 (azomethine ylide **1**) to −4.24 (azide **7**) eV. Many of them are close to that of ethylene **9**, −3.37 eV, suggesting that the corresponding 32CA reactions will have non-polar processes. On the other hand, these values are higher than electronic chemical potentials μ of DCE **10**, −5.64 eV, indicating that in these 32CA reactions the GEDT will flux from the TACs, acting as the nucleophilic species, towards DCE **10**, acting as the electrophilic species. Therefore, the corresponding polar 32CA reactions will be classified as FEDT reactions[9].

Two appealing conclusions can be obtained from the electronic chemical potentials μ of these TACs: i) the electronic chemical potentials μ decrease with the increase of the number of electronegative atoms present in the TAC; and ii) considering the pairs of B-TACs and L-TACs, B-TACs present higher μ than L-TACs.

The chemical hardness [29] η of the TACs ranges from 4.47 (azomethine ylide **1**) to 7.92 (nitrile oxide **8**) eV. The same trend observed in the increase of the electronic chemical potentials μ is observed in the increase of the chemical hardnesses η. Except diazomethane **61**, L-TACs are harder species than B-TACs, suggesting more resistance of the former against perturbations. Interestingly, a correlation between the chemical

Preprints (www.preprints.org) | NOT PEER-REVIEWED | Posted: 18 May 2021 doi:10.20944/preprints202105.0421.v1

hardness and the type of electronic structure of the TAC can be noticed, in such a manner that the chemical hardness increases in the order *pseudodiradical* < *pseudo(mono)radical* < carbenoid < zwitterionic.

The electrophilicity ω indices [30] of the TACs range from 0.37 (azomethine ylide **1**) to 1.40 (diazomethane **61**) eV. TACs **3**, **4**, **61**, **62** and **7** are classified as moderate electrophiles, while TACs **1**, **2**, **5** and **8** are classified as marginal electrophiles [25]; consequently, they will not have any tendency to participate in polar reactions towards a nucleophilic ethylene. On the other hand, the nucleophilicity *N* indices [31] of the TACs range from 1.62 (azide **7**) to 5.07 (azomethine ylide **1**) eV. Except for L-TACs azide **7** and nitrile oxide **8**, the other TACs are classified as moderate or strong nucleophiles. Note that azomethine ylide **1** is classified as a supernucleophile [32]. Consequently, at least four TACs, **1**, **2**, **5** and **61**, will participate in polar 32CA reactions towards electrophilic ethylenes. In general, B-TACs are more nucleophilic that their L-TAC counterparts.

As for ethylene **9** and DCE **10**, their electrophilicity ω indices are 0.73 and 2.82 eV, respectively, indicating what while ethylene **9** cannot participate in polar reactions towards these TACs, DCE **10** will participate as a strong electrophile, and in particular, its reactions with B-TACs **1** and **2**, and L-TACs **5** and **61** are expected to have a high polar character, in clear agreement with the analysis of the GEDT at the corresponding more favourable TSs (see section 3.3).

In polar cycloaddition reactions involving non-symmetric reagents, the preferred reaction path is that involving the most favourable two-center electrophilic/nucleophilic interaction between the nucleophilic-electrophilic pairs [33]. In this context, the electrophilic P_k^+ and nucleophilic P_k^- Parr functions [34], derived from the excess of spin electron density reached via the GEDT process from the nucleophile towards the electrophile, have shown to be the most accurate and insightful tools for the study of the local reactivity in polar and ionic processes. Hence, in order to investigate the effect of the dehydrogenation of B-TACs on the local reactivity of L-TACs, the nucleophilic P_k^- Parr functions of TACs **1-8** were analysed together with the electrophilic P_k^+ Parr functions of DCE **10** (see Figure 2).

Preprints (www.preprints.org) | NOT PEER-REVIEWED | Posted: 18 May 2021 doi:10.20944/preprints202105.0421.v1

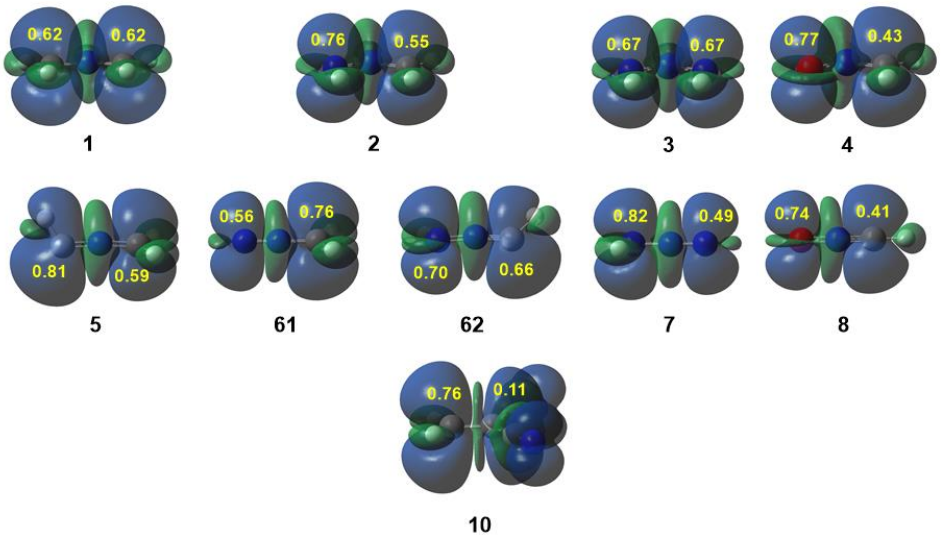

Figure 2. 3D representation of the Mulliken atomic spin density maps of radical cations (**1-8**)$^{\cdot+}$ and radical anion **10**$^{\cdot-}$ together with the nucleophilic P_k^- Parr functions of TACs **1-8** and the electrophilic P_k^+ Parr functions of DCE **10**.

When the changes in the Parr functions were analysed by pairs of B-TACs and L-TACs, no noticeable trend could be found. In non-symmetric B-TACs **2** and **4** and L-TACs **5**, **62** and **8**, the more electronegative heteroatom holds the higher nucleophilic P_k^- Parr function (see Figure 2). Upon dehydrogenation, the most nucleophilic center in L-TACs is the non-dehydrogenated site, except in nitrile ylide **5**, where the carbenoid CH carbon is more nucleophilic than the methylene CH_2 one. Only in pair azomethine imine **2** / diazomethane **61**, the Parr functions predict an opposite regioselectivity.

*3.3. Study of the reaction paths associated with the 32CA reactions of TACs **1-8** with ethylene **9** and with the electrophilic DCE **10***

*3.3.1. Study of the 32CA reactions with ethylene **9***

In order to investigate the effect of the polar character in the reactions of B-TACs and L-TACs, the non-polar 32CA reactions of TACs **1-8** with ethylene **9** were studied first. Note that ethylene **9** is a marginal electrophile and a marginal nucleophile, not participating in polar reactions (see Table 1). Due to the symmetry of ethylene **9**, there is only one single reaction path for each of the nine 32CA reactions (see Scheme 4). Analysis of the stationary points indicate that all 32CA reactions take place through a one-step

Preprints (www.preprints.org) | NOT PEER-REVIEWED | Posted: 18 May 2021 doi:10.20944/preprints202105.0421.v1

mechanism. The gas phase relative energies of the stationary points involved in every 32CA reaction are given in Table 2, while the total electronic energies are given in Table S1 in Supplementary Material.

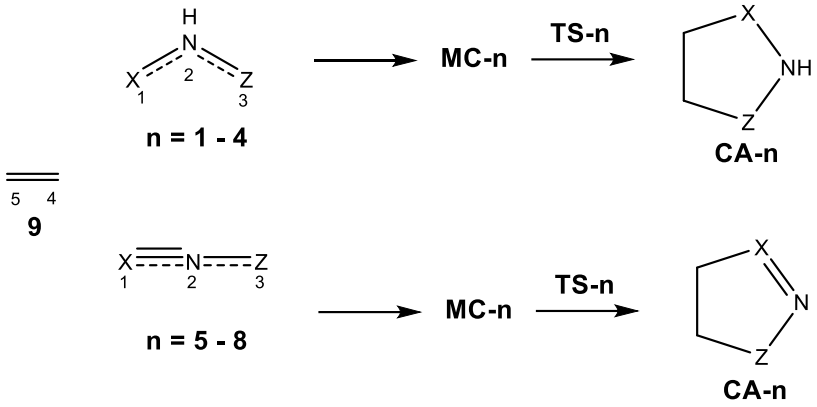

Scheme 4. Simplest 32CA reactions of TACs **1-8** with ethylene **9**.

Analysis of the potential energy surface associated with these 32CA reactions allows finding a series of molecular complexes (MCs) in an early stage of the reactions in which both reagents are weakly bound by non-covalent interactions. These MCs are between 0.8 (**MC-62**) and 3.3 (**MC-4**) kcal·mol^{-1} more stable than the separated reagents (see Scheme 4 and Table 3). The relative energies of the TSs associated with the 32CA reactions of B-TACs **1-4** with ethylene **9**, with respect the separated reagents, range from 0.1 (**TS-1**) to 15.5 (**TS-3**) kcal·mol^{-1}, while those associated with the 32CA reactions of L-TACs **5-8** range from 7.2 (**TS-5**) to 21.1 (**TS-7**) kcal·mol^{-1} (see Table 3). The relative energies of the corresponding cycloadducts range from −81.4 (**CA-5**) to −30.0 (**CA-7**) kcal·mol^{-1}, the reactions being strongly exothermic. The relative energy difference between the TSs associated with the 32CA reactions of each pair of B- and L-TACs are: 7.1 (*pdr* **1**/*cb* **5**), 9.9 (*pmr* **2**/*pmr* **61**), 1.6 (*pmr* **2**/*cb* **62**), 5.6 (*zw* **3**/*zw* **7**) and 3.8 (*zw* **4**/*zw* **8**) kcal·mol^{-1}.

Table 3. MPWB1K/6-311G(d,p) gas phase relative electronic energies, in kcal·mol^{-1}, with respect to the separated reagents, of the stationary points involved in the 32CA reactions of TACs **1-8** with ethylene **9**.

TAC	**MC-n**	**TS-n**	**CA-n**
1	-1.8	0.1	-77.8
2	-2.3	6.4	-59.4
3	-2.9	15.5	-43.2
4	-3.3	11.8	-41.0

Preprints (www.preprints.org) | NOT PEER-REVIEWED | Posted: 18 May 2021 doi:10.20944/preprints202105.0421.v1

5	-1.2	7.2	-81.5
61	-1.0	16.3	-42.6
62	-0.8	8.0	-68.9
7	-3.1	21.1	-30.0
8	-1.5	15.6	-50.8

Some appealing conclusions can be obtained from these data: i) the TSs of the L-TACs are by between 1.6 (**62**) and 9.9 (**61**) kcal·mol^{-1} higher in energy than those of the B-TACs; ii) the reactivity among B-TACs follows the trend *pdr* > *pmr* > *zw*, as previously suggested [5], while among L-TACs, the reactivity decreases in the order *cb* > *zw* > *pmr*. Note that the reactivity of diazomethane **61** seems to be an exception; and iii) except *pseudo(mono)radical* **61**, only zwitterionic TACs present a low reactivity towards ethylene **9**; the activation energies of the *zw-type* 32CA reactions are higher than 11.8 kcal·mol^{-1} (nitrone **4**). Note that the low reactivity of *pseudo(mono)radical* diazomethane **61**, 16.3 kcal·mol^{-1}, might be considered an exception.

The gas phase optimized geometries of the TSs involved in the 32CA reactions of TACs **1-8** with ethylene **9** are shown in Figure 3 together with the distances between the four interacting centers. Some appealing conclusions can be obtained from these geometrical parameters: i) except **TS-1** and **TS-3**, which are completely synchronous, the other seven TSs are geometrically low asynchronous. The most asynchronous TS is **TS-8**, with Δd = 0.14 Å, while the least asynchronous one is **TS-7**, with Δd = 0.02 Å; ii) the geometries of **TS-8**, **TS-61** and **TS-62**, associated with L-TACs **8**, **61** and **62**, are more asynchronous than **TS-4** and **TS-2**, associated with their B-TAC counterparts **4** and **2**. Given the complete synchronicity of **TS-1** and **TS-3**, it could be considered that the TSs associated with L-TACs are in general more asynchronous than those associated with B-TACs; iii) five of the nine TSs agrees with Hammond's principle [35], however, Hammond's correlation between distances and reactivity does not hold for the TSs of L-TACs **61** and **8**, and B-TACs **3** and **4**; and finally, iv) the shorter distance in non-symmetric TSs corresponds with that involving the participation of the most nucleophilic center of the TAC except for **TS-62** and **TS-8**.

Preprints (www.preprints.org) | NOT PEER-REVIEWED | Posted: 18 May 2021 doi:10.20944/preprints202105.0421.v1

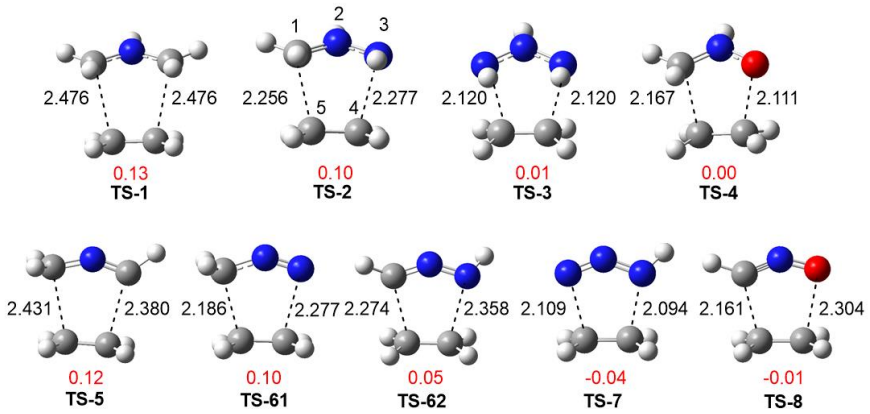

Figure 3. MPWB1K/6-311G(d,p) gas phase optimized geometries of the TSs involved in the 32CA reactions of TACs **1-8** with ethylene **9**. Distances are given in angstroms, Å, while the GEDT values computed at the TAC framework, in red, are given in average number of electrons, e.

The polar character of the nine 32CA reactions involving ethylene **9** was checked by computing the GEDT at every TS (see Figure 3). The GEDT values given in Figure 3 indicate that five of the nine reactions are non-polar, with absolute GEDT values lower than 0.05 e, while four reactions are low-polar, with GEDT values between 0.10 and 0.13 e. It is worth mentioning that these values over 0.10 e are not the consequence of favourable nucleophilic/electrophilic interactions [33]. Consequently, these GEDT values confirm the general low polar character of 32CA reactions involving the poor electrophilic ethylene **9**. The non-polar reactions correspond to those involving B-TACs **3** and **4**, and L-TACs **8** and **62**, with GEDT values ca. 0 e. When the GEDT values were analysed by pairs of TSs of B-TACs and L-TACs, no significant changes can be observed. Only the polar character at **TS-62**, involving L-TAC nitrile imine **62**, is notably lower than at **TS-2**, involving its B-TAC partner azomethine imine **2**.

*3.3.2. Study of the 32CA reactions with electrophilic DCE **10***

Due to the non-symmetry of TACs **2**,**4-8**, the 32CA reactions of these TACs with DCE **10** can take place along two competitive regioisomeric paths, labelled *meta* and *ortho* (see Scheme 5). While the *ortho* reaction paths involve the Z3–C4 interaction, the *meta* ones are involve the X1–C4 one. In every TAC, Z3 labels the most electronegative atom. Due to the symmetry of B-TACs **1** and **3**, only one single reaction path is possible in the corresponding 32CA reactions. Analysis of the stationary points found along each reaction path indicate that all 32CA reactions take place through a one-step mechanism

Preprints (www.preprints.org) | NOT PEER-REVIEWED | Posted: 18 May 2021 doi:10.20944/preprints202105.0421.v1

(see Scheme 5). The gas phase relative energies of the stationary points involved in every 32CA reaction are given in Table 4, while the total electronic energies are given in Table S2 in Supplementary Material.

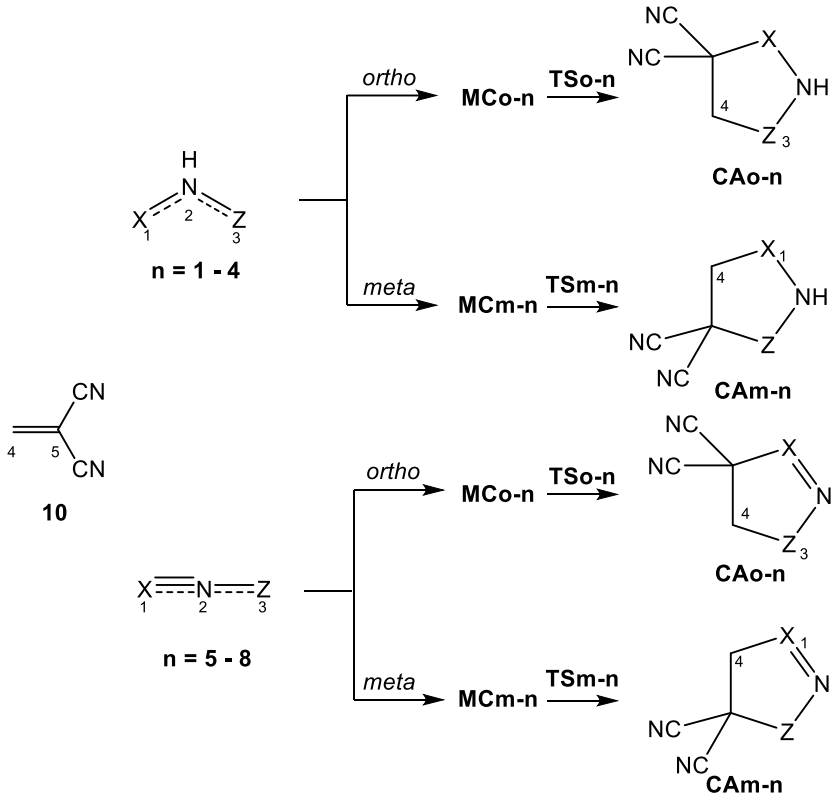

Scheme 5. Regioisomeric reaction paths associated with the 32CA reactions between TACs **1-8** and DCE **10**.

The analysis of the potential energy surface associated to these 32CA reactions allows finding a series of MCs in an early stage of the reactions in which both reagents are weakly bound by non-covalent interactions. These MCs are between 2.5 (**MCm-7**) and 9.0 (**MCo-4**) kcal·mol^{-1} more stable than the separated reagents (see Scheme 4 and Table 3). The relative energies of the TSs associated with the more favourable regioisomeric reaction paths range between –7.4 (**TSm-2**) and 5.9 (**TSm-3**) kcal·mol^{-1} for B-TACs **1-4**, and between –6.3 (**TSm-5**) and 21.9 (**TSm-7**) kcal·mol^{-1} for L-TACs **5-8**, with respect to the separated reagents. The reactions are exothermic by between 18.6 (**CAo-7**) and 76.6 (**CAm-1**) kcal·mol^{-1}. These data show the highly variable reactivity among TACs.

Preprints (www.preprints.org) | NOT PEER-REVIEWED | Posted: 18 May 2021 doi:10.20944/preprints202105.0421.v1

Table 4. MPWB1K/6-311G(d,p) gas phase relative electronic energies, in kcal·mol^{-1}, with respect to the separated reagents, of the stationary points involved in the 32CA reactions of TACs **1-8** with DCE **10**.

	ortho			*meta*		
TAC	**MCo-n**	**TSo-n**	**CAo-n**	**MCm-n**	**TSm-n**	**CAm-n**
1 *pdr*	-	-	-76.5			
2 *pmr*	-8.3	-7.4	-49.6	-5.9	-4.6	-53.6
3 *zw*	-4.0	5.9	-36.9			
4 *zw*	-7.8	-0.3	-36.5	-9.0	5.1	-31.8
5 *cb*	-6.9	-6.3	-76.1	-4.2	-1.8	-73.8
61 *pmr*	-4.0	11.3	-34.2	-2.6	4.6	-31.2
62 *cb*	-5.2	1.0	-60.9	-4.8	0.2	-61.1
7 *zw*	-2.5	21.9	-19.0	-5.6	16.4	-18.6
8 *zw*	-4.0	15.3	-38.3	-1.5	13.6	-38.3

Some appealing conclusions can be obtained from these energies: i) five of the fifteen TSs are located below the separated reagents. However, if the formation of the corresponding MCs is considered, all activation energies become positive; ii) the high reactivity of supernucleophilic azomethyne ylide **1** makes the 32CA reaction towards electrophilic DCE **10** barrierless; neither **MCo-1** nor **TSo-1** can be found as a stationary point on the PES; iii) the activation energies of these 32CA reactions, with respect to the corresponding MCs, range from 0.6 (**TSm-5**) to 22.0 (**TSo-7**); iv) considering the electronic structure of TACs, the reactivity among B-TACs decreases in the order *pdr* (**1**) > *pmr* (**2**) > *zw* (**3**, **4**), while that among L-TACs decreases in the order *cb* (**5**, **62**) > *pmr* (**61**) > *zw* (**6**, **8**), in agreement with the expected trend; v) in general, while B-TACs are *meta* regioselective, L-TACs are *ortho* regioselective except carbenoid nitrile ylide **5**. Consequently, considering the B-TAC/L-TAC pairs, a change of the *meta*/*ortho* regioselectivity is observed; vi) the regioselectivity of these 32CA reactions ranges from 0.8 (**TSo-62**) to 6.7 (**TSo-61**) kcal·mol^{-1}. The 32CA reactions of B-TAC **4** and L-TACs **61** and **8** are completely regioselective; vii) except for L-TAC **7**, the strong exothermic character of these 32CA reactions, higher than 31 kcal·mol^{-1} (**CAo-61**), makes them irreversible; viii) the Parr functions correctly predict the computed regioselectivities except in the reactions of L-TACs nitrile imine **62** and nitrile oxide **8**; ix) the relative energies of the more favourable TSs of the reactions of L-TACs **5-8** are by between 7.8 (**62**) and 13.9 (**8**) kcal·mol^{-1} higher than those of the corresponding B-TAC partners **1-4**, indicating, again, the higher reactivity of the latter; and finally, x) when the activation

Preprints (www.preprints.org) | NOT PEER-REVIEWED | Posted: 18 May 2021 doi:10.20944/preprints202105.0421.v1

energies associated with the 32CA reactions of TACs **1-8** with both ethylene **9** and DCE **10** are compared, it is found that those involving electrophilic DCE **10** are by between 2.0 (**TSo-8)** and 10.1 (**TSo-61**) kcal·mol^{-1} lower than those involved in the reactions with ethylene **9**. In addition, the higher reactivity of B-TACs over L-TACs is enhanced in polar reactions.

The gas phase optimized geometries of the TSs associated with the *ortho* regioisomeric reaction paths of the 32CA reactions between TACs **1-8** and DCE **10** are displayed in Figure 4, while those associated with the *meta* regioisomeric reaction path are shown in Figure 5. The following conclusions can be obtained from the geometrical parameters: i) the asynchronicity ranges from 0.20 (**TSo-5**) to 0.81(**TSm-3**) Å; ii) in general, the *ortho* regioisomeric **TSo-n** associated with the B-TACs are more asynchronous than the **TSm-n** ones, while the *meta* regioisomeric **TSm-n** associated with the L-TACs are more asynchronous than the **TSo-n** ones. Consequently, a change of the asynchronicity is found between B-TACs and L-TACs, in agreement with same energy change; iii) at the fifteen TSs, the Z3(X1)–C4 distance involving the most electrophilic center of DCE **10** is shorter than the X1(Z3)–C5 one [34]; and iv) the more favorable TSs of the 32CA reactions of TACs **1-8** with DCE **10** are much more asynchronous, by between 0.26 (nitrile oxide **2**) and 0.80 (azimine **8**) Å more, than those of the corresponding 32CA reactions with ethylene **9**, due to the high polar character of the former (see later).

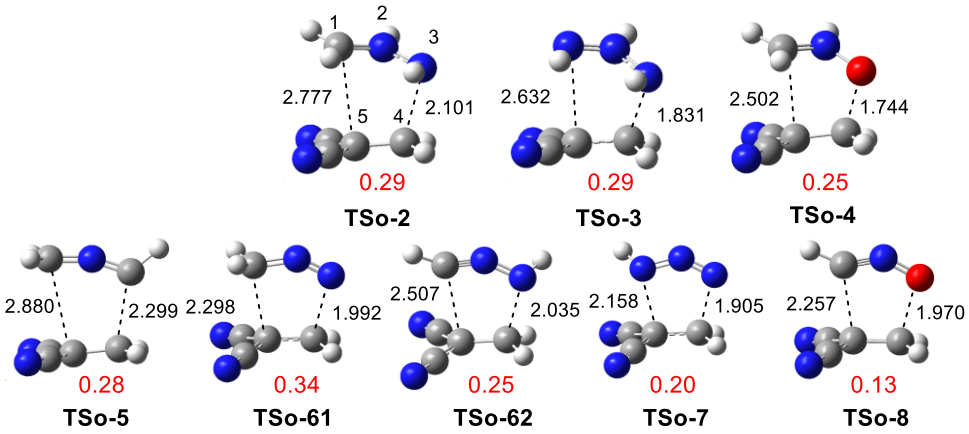

Figure 4. MPWB1K/6-311G(d,p) gas phase optimized geometries of the TSs associated with the *ortho* regiosimeric path of the 32CA reactions between TACs **1-8** and DCE **10**. Distances are given in angstroms, Å, while the GEDT values computed at the TAC framework, in red, are given in average number of electrons, e.

Preprints (www.preprints.org) | NOT PEER-REVIEWED | Posted: 18 May 2021 doi:10.20944/preprints202105.0421.v1

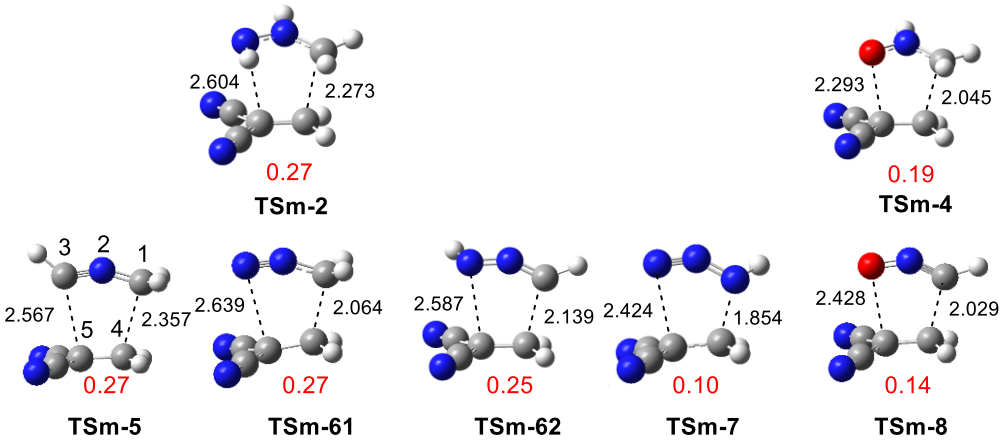

Figure 5. MPWB1K/6-311G(d,p) gas phase optimized geometries of the TSs associated with the *meta* regioisomeric path of the 32CA reactions between TACs **1-4,6,7** and DCE **10**. Distances are given in Angstroms, Å, while the GEDT values computed at the TAC framework, in red, are given in average number of electrons, e.

The polar character of the 32CA reactions of TACs **1-8** with DCE **10** was established by means of the GEDT taking place at the TSs, whose values are gathered in Figures 4 and 5. The GEDT taking place from the nucleophilic TAC framework to the electrophilic DCE one ranges from 0.10 (**TSm-7**) to 0.34 (**TSm-61**) e. Some conclusions arise from these values: i) except the 32CA reaction of nitrile oxide **8**, the rest of the 32CA reactions with DCE **10** have a high polar character, in agreement with the moderate to strong nucleophilicity of the TACs and the strong electrophilicity of DCE **10** (see section 3.1); ii) these 32CA reactions are classified as FEDF reactions, in clear agreement with the analysis of the CDFT indices; iii) these values are by between 0.08 (nitrone **4**) and 0.28 (azimine **3**) e higher than those associated with the TSs of the corresponding non-polar 32CA reactions with ethylene **9**; iv) in general, the TSs associated with the two *meta* and *ortho* regioisomeric reaction paths have similar GEDT values. Only in the reactions of diazomethane **61** and azide **7**, the GEDT is 0.07 and 0.10 e higher along the preferred *ortho* path; and finally, i) there is no clear trend between the GEDT and the electronic structure of TACs, considering the latter either geometrically or topologically.

4. Conclusions

The 32CA reactions of a series of five pairs of B-TACs and L-TACs with ethylene **9** and electrophilic DCE **10** have been studied within the MEDT at the MPWB1K/6-311G(d,p) computational level in order to understand how the dehydrogenation of B-TACs changes the electronic structure and reactivity of the L-TAC counterparts.

Preprints (www.preprints.org) | NOT PEER-REVIEWED | Posted: 18 May 2021 doi:10.20944/preprints202105.0421.v1

ELF topological analysis of the electronic structure of the nine TACs indicates that while the *pseudodiradical* and *pseudoradical* structures of B-TACs **1** and **2**, respectively, change to a carbenoid structure at L-TACs **5** and **62**, TACs **3** and **4** keep their zwitterionic structure at L-TACs **7** and **8**.

Analysis of the CDFT indices of the nine TACs indicates that while they have a moderate or marginal electrophilic character, thus being not able to participate in polar reactions with nucleophilic ethylenes, four of them have a strong nucleophilic character, thus participating in polar reactions towards electrophilic ethylenes such as DCE **10**. In non-symmetric TACs **2**, **4**, **5**, **62** and **8**, the more electronegative center holds the higher nucleophilic P_k^- Parr function.

The activation energies of the non-polar 32CA reactions of the nine TACs towards ethylene **9** range from 0.1 to 21.1 kcal·mol^{-1}. In general, L-TACs are less reactive than B-TACs. The TSs associated with the 32CA reactions of L-TACs are in general less asynchronous than the TSs associated with the B-TACs. These 32CA reactions have low polar character, such as those involving TACs **1**, **2**, **61**, **10**, or even non-polar character, such as those involving TACs **3**, **4**, **62**, **7** and **8**.

The activation energies of the polar 32CA reactions of the nine TACs towards DCE **10** range from 0.5 to 22.0 kcal·mol^{-1}. The activation energies of the TSs involved in the 32CA reactions of the four strongest nucleophilic TACs with DCE **10** are by between 4.3 and 9.1 kcal·mol^{-1} lower than those involved in the 32CA reactions with ethylene **9**. In general, B-TACs are more reactive than the L-TAC counterparts as a consequence of the more nucleophilic character of the former. A change of the regioselectivity is found in these polar 32CA reactions; in general, while B-TACs are *ortho* regioselective, L-TACs are *meta* regioselective. The Parr functions perform well in predicting the computed regioselectivity in seven of the nine polar reactions.

Analysis of the geometrical parameters indicates that at all TSs the distance involving the most electrophilic C4 carbon of DCE **10** is shorter than that involving the C5 one. A change of the asynchronicity is found between B-TACs and L-TACs.

Except the 32CA reaction of nitrile oxide **8**, the rest of the 32CA reactions with DCE **10** have a high polar character, in agreement with the moderate to strong nucleophilicity of the TACs and the strong electrophilicity of DCE **10**. These 32CA reactions are classified as FEDF reactions. There is no clear trend between the GEDT and

the electronic structure of TACs, however it is noticed that the polar character enhances even more the higher reactivity of B-TACs over L-TACs.

In this MEDT study, the structural and reactivity differences between B-TACs and L-TACs are examined for the first time entirely by means of the electron density as the only physical entity responsible for the chemical behaviour of these species participating in 32CA reactions, showing proof for the higher reactivity of B-TACs vs L-TACs as well as their different regioselectivity.

Author Contributions: M.R.G headed the subject, wrote the manuscript and performed calculations; L.R.D. headed the subject, wrote the manuscript and performed calculations; and F.G. performed calculations and wrote the manuscript.

Acknowledgments: This work has been supported by the European Union's Horizon 2020 research and innovation programme under the Marie Skłodowska-Curie grant agreement No. 846181 (MRG). This work has also received funding from the Ministerio de Ciencias, Innovación y Universidades of the Spanish Government, project PID2019-110776GB00 (AEI/FEDER, UE).

Conflicts of interest: There are no conflicts to declare.

References

(1) Moss, G. P.; Smith, P. A. S.; Tavernier, D. Pure Appl. Chem. 1995, 67, 1307.

(2) Carruthers, W. Cycloaddition Reactions in Organic Synthesis; Pergamon: Oxford,1990.

(3) Padwa, A. 1,3-Dipolar Cycloaddition Chemistry; Wileynterscience: New York, 1984; Vol. 1-2.

(4) Domingo, L.R. Molecular electron density theory: a modern view of reactivity in organic chemistry. *Molecules* **2016**, *21*, 1319.

(5) Ríos-Gutiérrez, M.; Domingo, L. R. Unravelling the mysteries of the [3+2] cycloaddition reactions. *Eur. J. Org. Chem.* **2019**, 267–282.

(6) Domingo, L.R.; Sáez J.A., Understanding the mechanism of polar Diels–Alder reactions. *Org. Biomol. Chem.* **2009**, *7*, 3576-358.

(7) Domingo, L.R. A new C-C bond formation model based on the quantum chemical topology of electron density. *RSC Adv.* **2014**, *4*, 32415–32428.

(8) Domingo, L. R; Ríos-Gutiérrez, M.; Pérez. P. How does the global electron density transfer diminish activation energies in polar cycloaddition reactions? A Molecular Electron Density Theory study. *Tetrahedron 2017*, *73*, 1718-1724.

(9) Domingo, L.R.; Ríos-Gutiérrez, M.; Pérez, P. A Molecular Electron Density Theory Study of the Reactivity of Tetrazines in Aza-Diels-Alder Reactions. *RSC Adv.* **2020**, *10*, 15394–15405.

(10) Domingo, L.R.; Kula, K.; Ríos-Gutiérrez, M. Unveiling the Reactivity of Cyclic Azomethine Ylides in [3+2] Cycloaddition Reactions within the Molecular Electron Density Theory. *Eur. J. Org. Chem.* **2020**, 5938–5948

(11) Houk, K. N.; González, J.; Li, Y. Pericyclic reaction transition states: passions and punctilios, 1935-1995. *Acc. Chem. Res.* **1995**, *28*, 81-90.

(12) Sustmann, R.; Trill, H. Substituent Effects in 1,3-Dipolar Cycloadditions of Phenyl Azid *Angew. Chem. Int. Ed. Engl.* 1972, **11**, 838–840.

(13) Domingo, L.R.; Mar Ríos-Gutiérrez, M.; Silvi, B.; Pérez; P. The Mysticism of Pericyclic Reactions: A Contemporary Rationalisation of Organic Reactivity Based on Electron Density Analysis. *Eur. J. Org. Chem.* **2018**, 1107–1120.

(14) Zhao, Y.; Truhlar, D. G. Hybrid Meta Density Functional Theory Methods for Thermochemistry, Thermochemical Kinetics, and Noncovalent Interactions: The MPW1B95 and MPWB1K Models and Comparative Assessments for Hydrogen Bonding and van der Waals Interactions. *J. Phys. Chem. A.* **2004**, *108*, 6908-6918.

(15) Hehre, M.J.; Radom, L.; Schleyer, P.v.R.; Pople, J. Ab initio Molecular Orbital Theory, Wiley, New York, 1986.

(16) Schlegel, H.B. Optimization of equilibrium geometries and transition structures. *J. Comput. Chem.* **1982**, *3*, 214-218.

(17) Schlegel, H.B. In modern electronic structure theory, Yarkony, D.R., Ed., World Scientific Publishing, Singapore, 1994.

(18) Fukui, K. Formulation of the reaction coordinate. *J. Phys. Chem.* **1970**, *74*, 4161–4163.

(19) González, C.; Schlegel, H. B. Reaction path following in mass-weighted internal coordinates. *J. Phys. Chem.* **1990**, *94*, 5523–5527.

(20) González, C.; Schlegel, H. B. Improved algorithms for reaction path following: higher-order implicit algorithms. *J. Chem. Phys.* **1991**, *95*, 5853–5860.

(21) Becke, A.D. Edgecombe, K.E. A simple measure of electron localization in atomic and molecular-systems. *J. Chem. Phys.* **1990**, *92*, 5397-5403.

(22) Reed, A.E.; Weinstock, R.B.; Weinhold, F. Natural population analysis. *J. Chem. Phys.*, **1985**, *83*, 735-746.

(23) Reed, A.E.; Curtiss, L.A.; Weinhold, F. Intermolecular interactions from a natural bond orbital, donor-acceptor viewpoint. *Chem. Rev.* **1988**, *88*, 899-926.

(24) Parr, R.G.; Yang, W. Density functional theory of atoms and molecules, Oxford University Press, New York, 1989.

(25) Domingo, L.R.; Ríos-Gutiérrez, M.; Pérez, P. Applications of the conceptual density functional indices to organic chemistry reactivity. *Molecules* **2016**, *21*, 748.

(26) Gaussian 16, Revision A.03, Frisch, M.J.; Trucks, G.W.; Schlegel, H.B.; Scuseria, G.E.; Robb, M.A.; Cheeseman, J.R.; Scalmani, G.; Barone, V.; Petersson, G. A.; Nakatsuji, H.; et al. Gaussian, Inc., Wallingford CT, **2016**.

(27) Noury, S.; Krokidis, X.; Fuster, F.; Silvi, B. Computational tools for the electron localization function topological analysis. *Comput. Chem.* **1999**, *23*, 597-604.

(28) Huisgen, R. 1,3-Dipolar Cycloadditions. *Proc. Chem. Soc.* **1961**, 357.

(29) Parr, R.G.; Pearson, R.G. Absolute hardness: Companion parameter to absolute electronegativity. *J. Am. Chem. Soc.* **1983**, *105*, 7512-7516.

(30) Parr, R.G. Szentpaly, L.v.; Liu, S. Electrophilicity index. *J. Am. Chem. Soc.* **1999**, *121*, 1922-1924.

(31) Domingo, L.R.; Chamorro, E.; Pérez, P. Understanding the reactivity of captodative ethylenes in polar cycloaddition reactions. A theoretical study. *J. Org. Chem.* **2008**, *73*, 4615-4624.

(32) Chamorro, E.; Duque-Noreña, M.; Gutierrez-Sánchez, N.; Rincón, E.; Domingo, L. R. A close look to the oxaphosphetane formation along the Wittig reaction: A [2+2] cycloaddition? *J. Org. Chem.* **2020**, *85*, 6675−6686.

(33) Aurell, M.J.; Domingo, L.R.; Pérez, P., Contreras, R. A theoretical study on the regioselectivity of 1,3-dipolar cycloadditions using DFT-based reactivity indexes. *Tetrahedron* **2004**, *60*, 11503-11509.

(34) Domingo, L.R.; Pérez, P; Sáez, J.A. Understanding the local reactivity in polar organic reactions through electrophilic and nucleophilic Parr functions. *RSC Adv.* **2013**, *3*, 1486-1494.

(35) Hammond, G. S. A Correlation of Reaction Rates *J. Am. Chem Soc* **1955**, *77*, 334-338.